

Diffusion Actor-Critic with Entropy Regulator

**Yinuo Wang¹ Likun Wang¹ Yuxuan Jiang¹ Wenjun Zou¹ Tong Liu¹
Xujie Song¹ Wenxuan Wang¹ Liming Xiao² Jiang Wu²
Jingliang Duan^{1,2*} Shengbo Eben Li^{1*}**

¹Tsinghua University ²University of Science and Technology Beijing

Abstract

Reinforcement learning (RL) has proven highly effective in addressing complex decision-making and control tasks. However, in most traditional RL algorithms, the policy is typically parameterized as a diagonal Gaussian distribution with learned mean and variance, which constrains their capability to acquire complex policies. In response to this problem, we propose an online RL algorithm termed diffusion actor-critic with entropy regulator (DACER). This algorithm conceptualizes the reverse process of the diffusion model as a novel policy function and leverages the capability of the diffusion model to fit multimodal distributions, thereby enhancing the representational capacity of the policy. Since the distribution of the diffusion policy lacks an analytical expression, its entropy cannot be determined analytically. To mitigate this, we propose a method to estimate the entropy of the diffusion policy utilizing Gaussian mixture model. Building on the estimated entropy, we can learn a parameter α that modulates the degree of exploration and exploitation. Parameter α will be employed to adaptively regulate the variance of the added noise, which is applied to the action output by the diffusion model. Experimental trials on MuJoCo benchmarks and a multimodal task demonstrate that the DACER algorithm achieves state-of-the-art (SOTA) performance in most MuJoCo control tasks while exhibiting a stronger representational capacity of the diffusion policy.

1 Introduction

Recently, deep reinforcement learning (RL) has emerged as an effective method for solving optimal control problems in the physical world [14, 28, 21, 24]. In most existing RL algorithms, the policy is parameterized as a deterministic function or a diagonal Gaussian distribution with the learned mean and variance [30, 31, 16, 10]. However, the theoretically optimal policy may exhibit strong multimodality, which cannot be well modeled by deterministic or diagonal Gaussian policies [42, 20, 44]. Restricted policy representation capabilities can make algorithms prone to local optimal solutions, damaging policy performance. For instance, in situations where two distinct actions in the same state yield approximately the same Q-value, the Gaussian policy approximates the bimodal action by maximizing the Q-value. This results in the policy displaying mode-covering behavior, concentrating high density in the intermediate region between the two patterns, which is inherently a low-density region with a lower Q-value. Consequently, modeling the policy with a unimodal Gaussian distribution is likely to significantly impair policy learning.

Lately, the diffusion model has become widely known as a generative model for its powerful ability to fit multimodal distributions [18, 34, 8]. It learns the original data distribution through the idea of stepwise addition and removal of noise and has excellent performance in the fields of image [45, 27] and video generation [9, 3]. The policy network in RL can be seen as a state-conditional generative model. Given the ability of diffusion models to fit complex distributions, there is increasing work on

*Corresponding author.

combining RL with diffusion models. Online RL learns policies by interacting with the environment [16, 31]. Offline RL, also known as batch RL, aims to effectively learn policies from previously collected data without interacting with the environment [1, 4]. In practical applications, many control problems have excellent simulators. At this time, using offline RL is not appropriate, as online RL with interaction capabilities performs better. Therefore, this paper focuses on how the diffusion model can be combined with online RL.

In this work, we propose diffusion actor-critic with entropy regulator (DACER), a generalized new approach to combine diffusion policy with online RL. Specifically, we base DACER on the denoising diffusion probabilistic model (DDPM) [18]. A recent work by He *et al.* [43] points out that the representational power of diffusion models stems mainly from the reverse diffusion processes, not from the forward diffusion processes. Inspired by this work, we reconceptualize the reverse process of the diffusion model as a novel policy approximator, leveraging its powerful representation capabilities to enhance the performance of RL algorithms. The optimization objective of this novel policy function is to maximize the expected Q-value. Maximizing entropy is important for policy exploration in RL, but the entropy of the diffusion policy is difficult to determine. Therefore, we choose to sample actions at fixed intervals and use a Gaussian mixture model (GMM) to fit the action distributions. Subsequently, We can calculate the approximate entropy of the policy in each state. The average of these entropies is then used as an approximation of the current diffusion policy entropy. Then, we use the estimated entropy to regulate the degree of exploration and exploitation of diffusion policy.

In summary, the key contributions of this paper are the following: 1) We propose to consider the reverse process of the diffusion model as a novel policy function. The objective function of the diffusion policy is to maximize the expected Q-value and thus achieve policy improvement. 2) We propose a method for estimating the entropy of diffusion policy. The estimated value is utilized to achieve an adaptive adjustment of the exploration level of the diffusion policy, thus improving the policy performance. 3) We evaluate the efficiency and generality of our method on the popular MuJoCo benchmarking. Compared with DDPG [32], TD3 [12], PPO [31], SAC [16], DSAC [11, 10], and TRPO [30], our approach achieves the SOTA performance. In addition, we demonstrate the superior representational capacity of our algorithm through a specific multi-goal task. 4) We provide the DACER code written in PyTorch and JAX in the attachment file to facilitate future researchers to follow our work.

Section 2 introduces and summarizes existing approaches to diffusion policy in offline RL and online RL, pointing out some of their problems. Section 3 provides an introduction to online RL and diffusion models. Our approach to combining diffusion policy with the mainstream actor-critic framework, as well as methods to enhance the performance of diffusion policy will be presented in section 4. The results of the experiments in the MuJoCo environment, the ablation experiments as well as the multimodality task will be presented in section 5. Section 6 provides the conclusions of this paper.

2 Related Work

Diffusion Policy in Offline RL Offline RL leverages pre-collected datasets for policy development, circumventing direct environmental interaction. Current offline RL research utilizing diffusion models as policy networks primarily adhere to the behavioral cloning framework [7, 25]. Within this framework, two main objectives emerge: performance enhancement and training efficiency improvement. For the former, Cheng *et al.* [6] proposed a Diffusion Policy, casting the policy as a conditional denoising diffusion process within the action space to accommodate complex multimodal action distributions. Wang *et al.* [42] introduced Diffusion-QL, which integrates behavior cloning via diffusion model loss with Q-learning for policy improvement. Ajay *et al.* [2] created Decision Diffusion, incorporating classifier-free guidance into the diffusion model to integrate trajectory information, such as rewards and constraints. Addressing the latter, Kang *et al.* [19] developed efficient diffusion policies (EDP), an evolution of Diffusion-QL. EDP accelerates training by utilizing initial actions from state-action pairs in the buffer and applying a one-step sample for final action derivation. Chen *et al.* [5] proposed a consistency policy that enhances diffusion algorithm efficiency through one-step action generation from noise during training and inference. Although Diffusion Policy’s powerful ability to fit multimodal policy distributions can achieve good performance in offline RL tasks, this method of policy improvement based on behavioral cloning cannot be directly transferred to online RL. In addition, the biggest challenge facing offline RL, the distribution shift

problem, has not been completely solved. This paper focuses on online RL, moving away from the framework of behavioral cloning.

Diffusion Policy in Online RL Online RL, characterized by real-time environment interaction, contrasts with offline RL’s dependence on pre-existing datasets. To date, only two studies have delved into integrating online RL with diffusion models. Yang *et al.* [44] pioneered this approach by using the action gradient method for action updates in replay buffers, facilitating diffusion policy improvement and theoretically proving its convergence. However, this method diverges from traditional policy evaluation and policy improvement in RL, incorporating changes to the core of RL that hinder compatibility with established algorithms and is also time-inefficient. Psenka *et al.* [29] introduced Q-score matching (QSM) for off-policy online RL, moving away from conventional behavioral cloning by leveraging the relationship between a score of policy and the action gradient Q-function in diffusion models. The QSM approach is also difficult to combine with existing RL algorithms. Because, in contrast with the traditional RL policy network that maximizes the expected reward, its objective function aims to minimize the discrepancy between the derivative of the Q function concerning action and the derivative of the log strategy probability concerning action. Moreover, the multimodal aspects of the diffusion policy remain underexplored. The performance of the above two methods in MuJoCo is lower than that of SAC, so we do not compare with them in experiments.

Our method is motivated to propose a diffusion policy that can be combined with most existing actor-critic frameworks. We first consider the reverse diffusion process of the diffusion model as a policy function with strong representational power. Then, we use the entropy estimation method to balance the exploration and utilization of diffusion policy and improve the performance of the policy.

Comparison with Diffusion-QL Diffusion-QL [42] made a successful attempt by replacing the diagonal Gaussian policy with a diffusion model. It also guides the updating of the policy by adding the normalized Q-value in the policy loss term. The main differences between our work and Diffusion-QL are as follows: 1) Diffusion-QL is still essentially an architecture for imitation learning, and policy updates are mainly motivated by the imitation learning loss term. 2) Our work adaptively regulates the standard deviation of random noise in the sampling process $\mathbf{a} = \mathbf{a} + \lambda\alpha \cdot \mathcal{N}(0, \mathbf{I})$, where α is a learned parameter, λ is a hyperparameter. This method effectively balances exploration and exploitation and subsequently enhances the performance of the diffusion policy. Ablation experiments provide evidence supporting these findings.

3 Preliminaries

3.1 Online Reinforcement Learning

In the conventional framework of RL, interactions between the agent and its environment occur in sequential discrete time steps. Typically, the environment is modeled as a Markov decision process (MDP) with continuous states and actions [37]. The environment provides feedback through a bounded reward function denoted by $r(s_t, a_t)$. The likelihood of transitioning to a new state based on the agent’s action is expressed by the probability $p(s_{t+1}|s_t, a_t)$. State-action pairs for the current and next steps are indicated as (s, a) and (s', a') . The decision-making of an agent at any state s_t is guided by a stochastic policy $\pi(a_t|s_t)$, which determines the probability distribution over feasible actions at that state.

In the realm of online RL, agents engage in real-time learning and decision-making through direct interactions with their environments. Such interactions are captured within a tuple (s_t, a_t, r_t, s_{t+1}) , representing the transition during each interaction. It is common practice to store these transitions in an experience replay buffer, symbolized as \mathcal{B} . Throughout the training phase, random samples drawn from \mathcal{B} produce batches of data that contribute to a more consistent training process. The fundamental aim of traditional online RL strategies is to craft a policy that optimizes the expected total reward:

$$J_\pi = \mathbb{E}_{(s_i \geq t, a_i \geq t) \sim \pi} \left[\sum_{i=t}^{\infty} \gamma^{i-t} r_i \right], \quad (1)$$

where $\gamma \in (0, 1)$ represents the discount factor. The Q-value for a state-action pair (s, a) is given by

$$Q(s, a) = \mathbb{E}_\pi \left[\sum_{i=t}^{\infty} \gamma^{i-t} r_i \right]. \quad (2)$$

RL typically employs an actor-critic framework [24, 23], which includes both a policy function, symbolized by π , and a corresponding Q-value function, noted as Q^π . The process of policy iteration is often used to achieve the optimal policy π^* , cycling through phases of policy evaluation and enhancement. In the policy evaluation phase, the Q-value Q^π is recalibrated according to the self-consistency requirements dictated by the Bellman equation:

$$Q^\pi(s, a) = r(s, a) + \gamma \mathbb{E}_{s' \sim p, a' \sim \pi} [Q^\pi(s', a')]. \quad (3)$$

In the policy improvement phase, an enhanced policy π_{new} is sought by optimizing current Q-value $Q^{\pi_{\text{old}}}$:

$$\pi_{\text{new}} = \arg \max_{\pi} \mathbb{E}_{s \sim d_\pi, a \sim \pi} [Q^{\pi_{\text{old}}}(s, a)]. \quad (4)$$

In practical applications, neural networks are often used to parameterize both the policy and value functions, represented by π_θ and Q_ϕ , respectively. These functions are refined through the application of gradient descent methods aimed at reducing the loss functions for both the actor, $\mathcal{L}_\pi(\theta)$, and the critic, $\mathcal{L}_q(\phi)$. These loss functions are structured based on the principles outlined in (4) and (3).

3.2 Diffusion Models

Diffusion models [33, 18, 35, 36] are highly effective generative tools. They convert data from its original distribution to a Gaussian noise distribution by gradually adding noise and then reconstruct the data by gradually removing this noise through a reverse process. This process is typically described as a continuous Markov chain: the forward process incrementally increases the noise level, while the reverse process involves a conditional generative model trained to predict the optimal reverse transitions at each denoising step. Consequently, the model reverses the diffusion sequence to generate data samples starting from pure noise.

Let us define $p_\theta(\mathbf{x}_0) := \int p_\theta(\mathbf{x}_{0:T}) d\mathbf{x}_{1:T}$, where $\mathbf{x}_1, \dots, \mathbf{x}_T$ denote latent variables sharing the same dimensionality as the data variable $\mathbf{x}_0 \sim q(\mathbf{x}_0)$, where $q(\mathbf{x}_0)$ means original data distribution. In a forward diffusion chain, the noise is incrementally introduced to the data $\mathbf{x}_0 \sim q(\mathbf{x}_0)$ across T steps, adhering to a predetermined variance sequence denoted by β_t , described as

$$q(\mathbf{x}_{1:T} | \mathbf{x}_0) = \prod_{t=1}^T q(\mathbf{x}_t | \mathbf{x}_{t-1}), \quad q(\mathbf{x}_t | \mathbf{x}_{t-1}) = \mathcal{N}(\mathbf{x}_t; \sqrt{1 - \beta_t} \mathbf{x}_{t-1}, \beta_t). \quad (5)$$

When $T \rightarrow \infty$, \mathbf{x}_T distributes as an isotropic Gaussian distribution [20]. The reverse diffusion process of the diffusion model can be represented as

$$p_\theta(\mathbf{x}_{0:T}) = p(\mathbf{x}_T) \prod_{t=1}^T p_\theta(\mathbf{x}_{t-1} | \mathbf{x}_t), \quad p_\theta(\mathbf{x}_{t-1} | \mathbf{x}_t) = \mathcal{N}(\mathbf{x}_{t-1}; \boldsymbol{\mu}_\theta(\mathbf{x}_t, t), \boldsymbol{\Sigma}_\theta(\mathbf{x}_t, t)), \quad (6)$$

where $p(\mathbf{x}_T) = \mathcal{N}(\mathbf{x}_T; \mathbf{0}, \mathbf{I})$ under the condition that $\prod_{t=1}^T (1 - \beta_t) \approx 0$.

4 Method

In this section, we detail the design of our diffusion actor-critic with entropy regulator (DACER). First, we consider the reverse diffusion process of the diffusion model as a new policy approximator, serving as the policy function in RL. Second, We directly optimize the diffusion policy using gradient descent, whose objective function is to maximize expected Q-values. This feature allows it to be integrated with mainstream RL algorithms that do not require entropy. However, the diffusion policy learned this way produces overly deterministic actions with poor performance. When attempting to integrate the maximization entropy RL framework, we find the entropy of the diffusion policy is difficult to analytically determine. Therefore, we use GMM to approximate the entropy of the diffusion policy, and then learn a parameter α based on it to adjust the exploration level of diffusion policy.

4.1 Diffusion Policy Representation

We use the reverse process of a conditional diffusion model as a parametric policy:

$$\pi_\theta(\mathbf{a}|\mathbf{s}) = p_\theta(\mathbf{a}_{0:T}|\mathbf{s}) = p(\mathbf{a}_T) \prod_{t=1}^T p_\theta(\mathbf{a}_{t-1}|\mathbf{a}_t, \mathbf{s}), \quad (7)$$

where $p(\mathbf{a}_T) = \mathcal{N}(0, \mathbf{I})$, the end sample of the reverse chain, \mathbf{a}_0 , is the action used for RL evaluation. Generally, $p_\theta(\mathbf{a}_{t-1}|\mathbf{a}_t, \mathbf{s})$ could be modeled as a Gaussian distribution $\mathcal{N}(\mathbf{a}_{t-1}; \boldsymbol{\mu}_\theta(\mathbf{a}_t, \mathbf{s}, t), \boldsymbol{\Sigma}_\theta(\mathbf{a}_t, \mathbf{s}, t))$. We choose to parameterize $\pi_\theta(\mathbf{a}|\mathbf{s})$ like DDPM [18], which sets $\boldsymbol{\Sigma}_\theta(\mathbf{a}_t, \mathbf{s}, t) = \beta_t \mathbf{I}$ to fixed time-dependent constants, and constructs the mean $\boldsymbol{\mu}_\theta$ from a noise prediction model as

$$\boldsymbol{\mu}_\theta(\mathbf{a}_t, \mathbf{s}, t) = \frac{1}{\sqrt{\alpha_t}} \left(\mathbf{a}_t - \frac{\beta_t}{\sqrt{1 - \bar{\alpha}_t}} \boldsymbol{\epsilon}_\theta(\mathbf{a}_t, \mathbf{s}, t) \right), \quad (8)$$

where $\alpha_t = 1 - \beta_t$, $\bar{\alpha}_t = \prod_{k=1}^t \alpha_k$, and $\boldsymbol{\epsilon}_\theta$ is a parametric model.

To obtain an action from DDPM, we need to draw samples from T different Gaussian distributions sequentially. The sampling process can be reformulated as

$$\mathbf{a}_{t-1} = \frac{1}{\sqrt{\alpha_t}} \left(\mathbf{a}_t - \frac{\beta_t}{\sqrt{1 - \bar{\alpha}_t}} \boldsymbol{\epsilon}_\theta(\mathbf{a}_t, \mathbf{s}, t) \right) + \sqrt{\beta_t} \boldsymbol{\epsilon}, \quad (9)$$

with the reparametrization trick, where $\boldsymbol{\epsilon} \sim \mathcal{N}(0, \mathbf{I})$, t is the reverse timestep from T to 0, $\mathbf{a}_T \sim \mathcal{N}(0, \mathbf{I})$.

4.2 Diffusion Policy Learning

In integrating diffusion policy with offline RL, policy improvement relies on minimizing the behavior-cloning term. However, in online RL, without a dataset to imitate, we discarded the behavior-cloning term and the imitation learning framework. In this study, the policy-learning objective is to maximize the expected Q-values of the actions generated by the diffusion network given the state:

$$\max_{\theta} \mathbb{E}_{\mathbf{s} \sim \mathcal{B}, \mathbf{a}_0 \sim \pi_\theta(\cdot|\mathbf{s})} [Q_\phi(\mathbf{s}, \mathbf{a}_0)]. \quad (10)$$

Unlike the traditional reverse diffusion process, our study requires recording the gradient of the whole process. The gradient of the Q-value function with respect to the action is backpropagated through the entire diffusion chain.

Policy improvement is introduced above; next, we introduce policy evaluation. The Q-value function is learned through a conventional approach, which involves minimizing the Bellman operator [13, 24, 37] with the double Q-learning trick [39]. We built two Q-networks $Q_{\phi_1}(\mathbf{s}, \mathbf{a})$, $Q_{\phi_2}(\mathbf{s}, \mathbf{a})$, and target network $Q_{\phi'_1}(\mathbf{s}, \mathbf{a})$, $Q_{\phi'_2}(\mathbf{s}, \mathbf{a})$. Then we give the objective function of policy evaluation, which is shown as

$$\min_{\phi_i} \mathbb{E}_{(\mathbf{s}, \mathbf{a}, \mathbf{s}') \sim \mathcal{B}} \left[\left(\left(r(\mathbf{s}, \mathbf{a}) + \gamma \min_{i=1,2} Q_{\phi'_i}(\mathbf{s}', \mathbf{a}') \right) - Q_{\phi_i}(\mathbf{s}, \mathbf{a}) \right)^2 \right], \quad (11)$$

where \mathbf{a}' is obtained by inputting the \mathbf{s}' into the diffusion policy, \mathcal{B} means replay buffer. Building on this, we employ the tricks in DSAC [11, 10] to mitigate the problem of Q-value overestimation.

The diffusion policy we construct can be directly combined with mainstream RL algorithms that do not require policy entropy. However, training with the above diffusion policy learning method suffers from overly deterministic policy actions, resulting in poor performance of the final diffusion policy. In the next section, we will propose entropy estimation to solve this problem and obtain diffusion policy with SOTA performance.

4.3 Diffusion Policy with Entropy

The diffusion policy's distribution lacks an analytic expression, so we cannot directly determine its entropy. However, in the same state, we can use multiple samples to obtain a series of actions. By fitting these action points, we can estimate the action distribution corresponding to the state.

In this paper, we use Gaussian mixture model (GMM) to fit the policy distribution. The GMM forms a complex probability density function by combining multiple Gaussian distributions, which can be represented as

$$\hat{f}(\mathbf{a}) = \sum_{k=1}^K w_k \cdot \mathcal{N}(\mathbf{a} | \boldsymbol{\mu}_k, \boldsymbol{\Sigma}_k), \quad (12)$$

where K is the number of Gaussian distributions, and w_k is the mixing weight of the k -th component, satisfying $\sum_{k=1}^K w_k = 1$, $w_k \geq 0$. $\boldsymbol{\mu}_k$, $\boldsymbol{\Sigma}_k$ are the mean and covariance matrices of the k -th Gaussian distribution, respectively.

For each state, we use a diffusion policy to sample N actions, $\mathbf{a}^1, \mathbf{a}^2, \dots, \mathbf{a}^N \in \mathcal{A}$. The Expectation-Maximization algorithm is then used to estimate the parameters of the GMM. In the expectation step, the posterior probability that each data point \mathbf{a}^i belongs to each component k is computed, denoted as

$$\gamma(\mathbf{z}_k^i) = \frac{w_k \cdot \mathcal{N}(\mathbf{a}^i | \boldsymbol{\mu}_k, \boldsymbol{\Sigma}_k)}{\sum_{j=1}^K w_j \cdot \mathcal{N}(\mathbf{a}^i | \boldsymbol{\mu}_j, \boldsymbol{\Sigma}_j)}, \quad (13)$$

where $\gamma(\mathbf{z}_k^i)$ denotes that under the current parameter estimates, the observed data \mathbf{a}^i come from the k -th component of the probability. In the maximization step, the results of the Eq. (13) calculations are used to update the parameters and mixing weights for each component:

$$w_k = \frac{1}{N} \sum_{i=1}^N \gamma(\mathbf{z}_k^i), \boldsymbol{\mu}_k = \frac{\sum_{i=1}^N \gamma(\mathbf{z}_k^i) \cdot \mathbf{a}^i}{\sum_{i=1}^N \gamma(\mathbf{z}_k^i)}, \boldsymbol{\Sigma}_k = \frac{\sum_{i=1}^N \gamma(\mathbf{z}_k^i) (\mathbf{a}^i - \boldsymbol{\mu}_k) (\mathbf{a}^i - \boldsymbol{\mu}_k)^T}{\sum_{i=1}^N \gamma(\mathbf{z}_k^i)}. \quad (14)$$

Iterative optimization continues until parameter convergence. Based on our experimental experience in the MuJoCo environments, a general setting of $K = 4$ provides a better fit to the action distribution.

According to Eq. (12), we can estimate the entropy of the action distribution corresponding to the state by

$$\mathcal{H}_s = - \sum_{k=1}^K w_k \log w_k + \sum_{k=1}^K w_k \cdot \frac{1}{2} \log ((2\pi e)^d |\boldsymbol{\Sigma}_k|), \quad (15)$$

where d is the dimension of action. Then, the mean of the entropy of the actions associated with the chosen batch of states is used as the estimated entropy $\hat{\mathcal{H}}$ of the diffusion policy.

Similar to maximizing entropy RL, we learn a parameter α based on the estimated entropy. We update this parameter using

$$\alpha \leftarrow \alpha - \beta_\alpha [\hat{\mathcal{H}} - \bar{\mathcal{H}}], \quad (16)$$

where $\bar{\mathcal{H}}$ is target entropy. Finally, we use $\mathbf{a} = \mathbf{a} + \lambda \alpha \cdot \mathcal{N}(0, \mathbf{I})$ to adjust the diffusion policy entropy during training, where λ is a hyperparameter and \mathbf{a} is the output of diffusion policy. Additionally, no noise is added during the evaluation phase. We summarize our implementation in Algorithm 1.

5 Experiments

We evaluate the performance of our method in some control tasks of RL within MuJoCo [38]. The benchmark tasks utilized in this study are depicted in Fig. 6, including Humanoid-v3, Ant-v3, HalfCheetah-v3, Walker2d-v3, InvertedDoublePendulum-v3, Hopper-v3, Pusher-v2, and Swimmer-v3. Moreover, we conducted experiments in a multi-goal task to demonstrate the excellent representational and exploratory capabilities of our diffusion policy. We also provide ablation studies on the critical components for better understanding. All baseline algorithms are available in GOPS [41], an open-source RL solver developed with PyTorch.

Baselines. Our algorithm is compared and evaluated against the six well-known model-free algorithms. These include DDPG [32], TD3 [12], PPO [31], SAC [16], DSAC [11, 10], and TRPO [30]. These baselines have been extensively tested and applied in a series of demanding domains.

Algorithm 1 diffusion actor-critic with entropy regulator for Online RL

Input: $\lambda, \theta, \phi_1, \phi_2, \phi'_1, \phi'_2, \alpha, \beta_q, \beta_\alpha, \beta_\pi$, and ρ

for each iteration **do**

- for** each sampling step **do**
- Sample $a \sim \pi_\theta(\cdot|s)$ by Eq. (7)
- Add noise $a = a + \lambda\alpha \cdot \mathcal{N}(0, I)$
- Get reward r and new state s'
- Store a batch of samples (s, a, r, s') in replay buffer \mathcal{B}

end for

for each update step **do**

- Sample data from \mathcal{B}
- Update critic networks using $\phi_i \leftarrow \phi_i - \beta_q \nabla_{\phi_i} \mathcal{L}_q(\phi_i)$ for $i = \{1, 2\}$
- Update diffusion policy network using $\theta \leftarrow \theta - \beta_\pi \nabla_\theta \mathcal{L}_\pi(\theta)$
- if** step mod 10000 == 0 **then**
- Estimate the entropy of diffusion policy $\hat{\mathcal{H}} = \mathbb{E}_{s \sim \mathcal{B}} [\mathcal{H}_s]$
- Update α using Eq. (16)
- Update target networks using $\phi'_i = \rho\phi'_i + (1 - \rho)\phi_i$ for $i = \{1, 2\}$

end for

end for

Experimental details. To ensure a fair comparison, we incorporated the diffusion policy as a policy approximation function within GOPS and implemented DACER with JAX, which improves training speed by 4-5 times compared to PyTorch while maintaining consistent performance. All algorithms and tasks use the same three-layer MLP neural network with GeLU [17] or Mish [26] activation functions, the latter used only for the noise prediction network in the diffusion policy. Initially, we encode timestep t into 16 dimensions using sinusoidal embedding [40], then merge this encoded result with the state s and action a_t during the current denoising step, and input it into the prediction noise network to generate the output. The impact of the reverse diffusion step size, T , on the experimental results will be examined in the ablation experiments. T is set to 20 for all experiments eventually. The Adam [22] optimization method is employed for all parameter updates. In this paper, the total training step size for all experiments is set at 1.5 million, with the results of all experiments averaged over five random seeds. The CPU used for the experiment is Xeon(R) Platinum 8352V, and the GPU is NVIDIA GeForce RTX 4090. Taking Humanoid-v3 as an example, the time taken to train 1.5 million in the JAX framework is 7 hours. More detailed hyperparameters are provided in Appendix A.2 due to space limits.

Evaluation Protocol. In this paper, we use the same assessment metrics as DSAC. For each seed, the metric is derived by averaging the highest return values observed during the final 10% of iteration steps in each run, with evaluations conducted every 15,000 iterations. Each assessment result is the average of ten episodes. The results from the five seeds are then aggregated to calculate the mean and standard deviation. Additionally, the training curves in Fig. 1 provide insights into the stability of the training process.

5.1 Comparative Evaluation

Each algorithm was subjected to five distinct tests, utilizing a variety of consistent random seeds to ensure robustness in the results. Fig. 1 and Table 1 display the learning curves and performance strategies, respectively. Our comprehensive findings reveal that across all evaluated tasks, the DACER algorithm consistently matched or surpassed the performance of all competing benchmark algorithms. Specifically, in the Humanoid-v3 scenario, our algorithm demonstrated enhancements of 124.7%, 111.1%, 73.1%, 27.3%, 9.8%, and 1131.9% over DDPG, TD3, PPO, SAC, DSAC, and TRPO, respectively.

5.2 Policy Representation Experiment

In this section, we conduct an experiment to confirm the representation capability of the diffusion policy. We use an environment called "Multi-goal" [15], as shown in Fig. 2, where the x -axis and

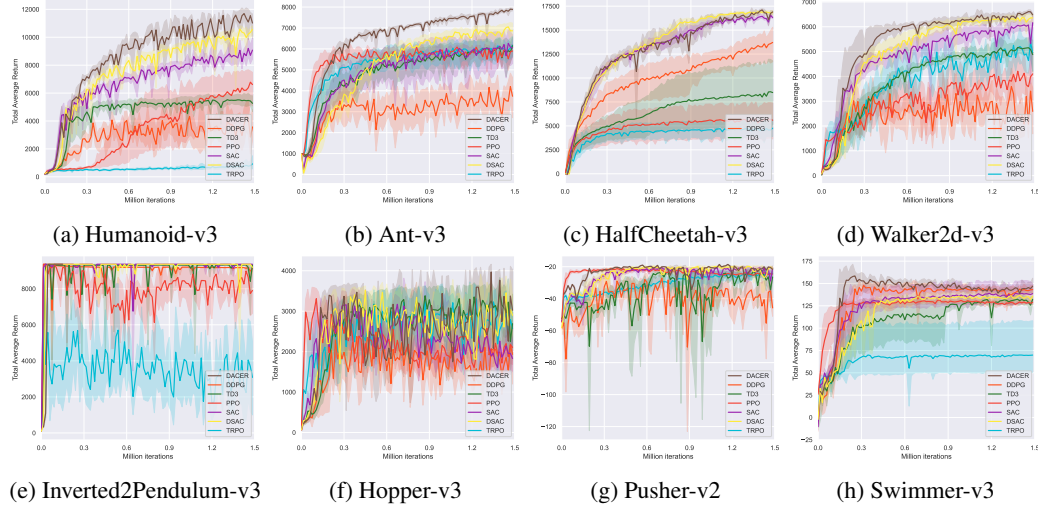


Figure 1: Training curves on benchmarks. The solid lines represent the mean, while the shaded regions indicate the 95% confidence interval over five runs. The iteration of PPO and TRPO is measured by the number of network updates.

TABLE 1

AVERAGE FINAL RETURN. COMPUTED AS THE MEAN OF THE HIGHEST RETURN VALUES OBSERVED IN THE FINAL 10% OF ITERATION STEPS PER RUN, WITH AN EVALUATION INTERVAL OF 15,000 ITERATIONS. THE MAXIMUM VALUE FOR EACH TASK IS BOLDED. \pm CORRESPONDS TO STANDARD DEVIATION OVER FIVE RUNS.

Task	DACER	DSAC	SAC	TD3	DDPG	TRPO	PPO
Humanoid-v3	11888 \pm 244	10829 \pm 243	9335 \pm 695	5631 \pm 435	5291 \pm 662	965 \pm 555	6869 \pm 1563
Ant-v3	7964 \pm 128	7086 \pm 261	6427 \pm 804	6184 \pm 486	4549 \pm 788	6203 \pm 578	6156 \pm 185
Halfcheetah-v3	17177 \pm 176	17025 \pm 157	16573 \pm 224	8632 \pm 4041	13970 \pm 2083	4785 \pm 967	5789 \pm 2200
Walker2d-v3	6701 \pm 62	6424 \pm 147	6200 \pm 263	5237 \pm 335	4095 \pm 68	5502 \pm 593	4831 \pm 637
Inverteddoublependulum-v3	9360 \pm 0	9360 \pm 0	9360 \pm 0	9347 \pm 15	9183 \pm 9	6259 \pm 2065	9356 \pm 2
Hopper-v3	4104 \pm 49	3660 \pm 533	2483 \pm 943	3569 \pm 455	2644 \pm 659	3474 \pm 400	2647 \pm 482
Pusher-v2	-19 \pm 1	-19 \pm 1	-20 \pm 0	-21 \pm 1	-30 \pm 6	-23 \pm 2	-23 \pm 1
Swimmer-v3	152 \pm 7	138 \pm 6	140 \pm 14	134 \pm 5	146 \pm 4	70 \pm 38	130 \pm 2

y-axis represent 2D states. In this setup, the agent is represented as a 2D point mass situated on a 7×7 plane. The objective for the agent is to navigate towards one of four symmetrically positioned points: $(0, 5)$, $(0, -5)$, $(5, 0)$, and $(-5, 0)$. Since the goal positions are symmetrically distributed at the four points, a policy with strong representational capacity should enable the Q-function to learn the four symmetric peaks across the entire state space. This result reflects the policy’s capacity for exploration in understanding the environment.

We compare the performance of DACER with DSAC, TD3, and PPO, as shown in Fig. 2. The results show that DACER’s actions are likely to point to the nearest peak in different states. DACER’s value function curve shows four symmetrical peaks, aligning with the previous analysis. Compared to DSAC, our method learns a better policy representation, mainly due to using a diffusion policy instead of an MLP. In contrast, TD3 and PPO generate more random actions with poorer policy representation, lacking the symmetrical peaks in their value function curves. Overall, our method demonstrates superior representational capability.

5.3 Ablation Study

In this section, we analyze why DACER outperforms all other baseline algorithms on MuJoCo tasks. We conduct ablation experiments to investigate the impact of the following three aspects on the performance of the diffusion policy: 1) whether adding Gaussian noise to the final output action of the diffusion policy; 2) whether the standard deviation of the added Gaussian noise can be adaptively

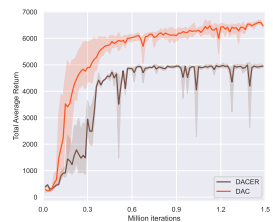


Figure 3: Training curves.

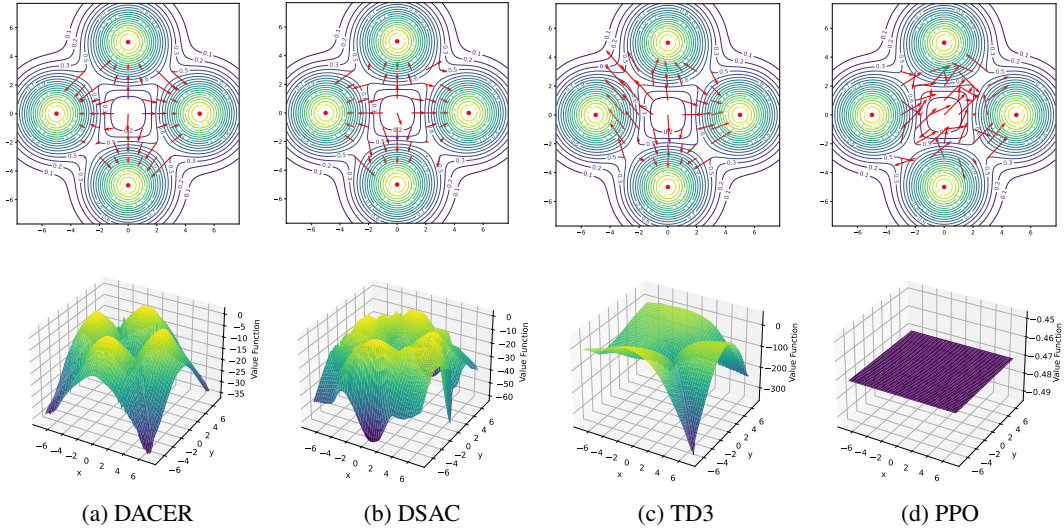


Figure 2: Policy representation comparison of different policies on a multimodal environment. The first row exhibits the policy distribution. The length of the red arrowheads denotes the size of the action vector, and the direction of the red arrowheads denotes the direction of actions. The second row shows the value function of each state point.

adjusted by estimated entropy; 3) different reverse diffusion step size T .

Only Q-learning. In section 4.2, we propose a method using the reverse diffusion process as a policy approximator, which can be combined with the non-maximizing entropy RL algorithm. However, the diffusion policy trained without entropy exhibits poor exploratory properties, leading to suboptimal performance. Using Walker2d-v3 as an example, we compared the training curves of this method with the DACER algorithm, as shown in Fig. 3.

Fixed and linear decay noise factor. In order to verify that using the estimated entropy to adaptively adjust the noise factor plays an important role in the final performance, we conducted the following two experiments in the Walker2d-v3 task: 1) Fixed noise factor to 0.1; 2) The noise factor starts from 0.27 and linearly decreases to 0.1 during the training process. These two values were chosen because the starting and ending noise factor for adaptive tuning in this setting is about in this range. As shown in Fig. 4, our method of adaptively adjusting the noise factor based on the estimated entropy achieves the best performance.

Diffusion steps. We further examined the performance of the diffusion policy as the number of diffusion timesteps T varied. We used the Walker2d-v3 task to plot training curves for $T = 10, 20$, and 30 , as shown in Fig. 5. Experimental results indicate that a larger number of diffusion steps does not necessarily lead to better performance. Excessive diffusion steps can cause gradient explosion, significantly reducing the performance of diffusion policy. After balancing performance and computational efficiency, we selected 20 diffusion steps for all experiments.

6 Conclusion

In this study, we propose the diffusion actor-critic with entropy regulator (DACER) algorithm, a novel RL method designed to overcome the limitations of traditional RL methods that use diagonal

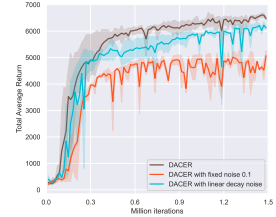


Figure 4: Training curves.

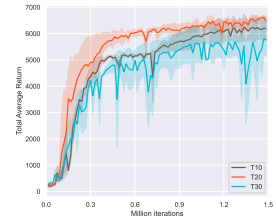


Figure 5: Training curves.

Gaussian distributions for policy parameterization. By utilizing the inverse process of the diffusion model, DACER effectively handles multimodal distributions, enabling the creation of more complex policies and improving policy performance. A significant challenge arises from the lack of analytical expressions to determine the entropy of a diffusion strategy. To address this, we employ GMM to estimate entropy, thereby facilitating the learning of a key parameter, α , which adjusts the exploration-exploitation balance by regulating the noise variance in the action output. Empirical tests on the MuJoCo benchmark and a multimodal task show the superior performance of DACER.

References

- [1] Rishabh Agarwal, Dale Schuurmans, and Mohammad Norouzi. An optimistic perspective on offline reinforcement learning. In *International Conference on Machine Learning*, pages 104–114. PMLR, 2020.
- [2] Anurag Ajay, Yilun Du, Abhi Gupta, Joshua Tenenbaum, Tommi Jaakkola, and Pulkit Agrawal. Is conditional generative modeling all you need for decision-making? *The Eleventh International Conference on Learning Representations*, 2023.
- [3] Andreas Blattmann, Tim Dockhorn, Sumith Kulal, Daniel Mendelevitch, Maciej Kilian, Dominik Lorenz, Yam Levi, Zion English, Vikram Voleti, Adam Letts, et al. Stable video diffusion: Scaling latent video diffusion models to large datasets. *arXiv preprint arXiv:2311.15127*, 2023.
- [4] David Brandfonbrener, Will Whitney, Rajesh Ranganath, and Joan Bruna. Offline rl without off-policy evaluation. *Advances in Neural Information Processing Systems*, 34:4933–4946, 2021.
- [5] Yuhui Chen, Haoran Li, and Dongbin Zhao. Boosting continuous control with consistency policy. *arXiv preprint arXiv:2310.06343*, 2023.
- [6] Cheng Chi, Siyuan Feng, Yilun Du, Zhenjia Xu, Eric Cousineau, Benjamin Burchfiel, and Shuran Song. Diffusion policy: Visuomotor policy learning via action diffusion. *arXiv preprint arXiv:2303.04137*, 2023.
- [7] Felipe Codevilla, Eder Santana, Antonio M López, and Adrien Gaidon. Exploring the limitations of behavior cloning for autonomous driving. In *Proceedings of the IEEE/CVF International Conference on Computer Vision*, pages 9329–9338, 2019.
- [8] Florinel-Alin Croitoru, Vlad Hondu, Radu Tudor Ionescu, and Mubarak Shah. Diffusion models in vision: A survey. *IEEE Transactions on Pattern Analysis and Machine Intelligence*, 2023.
- [9] Prafulla Dhariwal and Alexander Nichol. Diffusion models beat gans on image synthesis. *Advances in Neural Information Processing Systems*, 34:8780–8794, 2021.
- [10] Jingliang Duan, Yang Guan, Shengbo Eben Li, Yangang Ren, Qi Sun, and Bo Cheng. Distributional soft actor-critic: Off-policy reinforcement learning for addressing value estimation errors. *IEEE Transactions on Neural Networks and Learning Systems*, 33(11):6584–6598, 2021.
- [11] Jingliang Duan, Wenxuan Wang, Liming Xiao, Jiaxin Gao, and Shengbo Eben Li. Dsac-t: Distributional soft actor-critic with three refinements. *arXiv preprint arXiv:2310.05858*, 2023.
- [12] Scott Fujimoto, Herke Hoof, and David Meger. Addressing function approximation error in actor-critic methods. In *International Conference on Machine Learning*, pages 1587–1596. PMLR, 2018.
- [13] Scott Fujimoto, David Meger, and Doina Precup. Off-policy deep reinforcement learning without exploration. In *International Conference on Machine Learning*, pages 2052–2062. PMLR, 2019.
- [14] Yang Guan, Yangang Ren, Qi Sun, Shengbo Eben Li, Haitong Ma, Jingliang Duan, Yifan Dai, and Bo Cheng. Integrated decision and control: Toward interpretable and computationally efficient driving intelligence. *IEEE Transactions on Cybernetics*, 53(2):859–873, 2022.
- [15] Tuomas Haarnoja, Haoran Tang, Pieter Abbeel, and Sergey Levine. Reinforcement learning with deep energy-based policies. In *International Conference on Machine Learning*, pages 1352–1361. PMLR, 2017.
- [16] Tuomas Haarnoja, Aurick Zhou, Pieter Abbeel, and Sergey Levine. Soft actor-critic: Off-policy maximum entropy deep reinforcement learning with a stochastic actor. In *International Conference on Machine Learning*, pages 1861–1870. PMLR, 2018.
- [17] Dan Hendrycks and Kevin Gimpel. Gaussian error linear units (gelus). *arXiv preprint arXiv:1606.08415*, 2016.
- [18] Jonathan Ho, Ajay Jain, and Pieter Abbeel. Denoising diffusion probabilistic models. *Advances in Neural Information Processing Systems*, 33:6840–6851, 2020.
- [19] Bingyi Kang, Xiao Ma, Chao Du, Tianyu Pang, and Shuicheng Yan. Efficient diffusion policies for offline reinforcement learning. *Conference and Workshop on Neural Information Processing Systems*, 2023.

[20] Bingyi Kang, Xiao Ma, Chao Du, Tianyu Pang, and Shuicheng Yan. Efficient diffusion policies for offline reinforcement learning. *Advances in Neural Information Processing Systems*, 36, 2024.

[21] Elia Kaufmann, Leonard Bauersfeld, Antonio Loquercio, Matthias Müller, Vladlen Koltun, and Davide Scaramuzza. Champion-level drone racing using deep reinforcement learning. *Nature*, 620(7976):982–987, 2023.

[22] Diederik P Kingma and Jimmy Ba. Adam: A method for stochastic optimization. *arXiv preprint arXiv:1412.6980*, 2014.

[23] Vijay Konda and John Tsitsiklis. Actor-critic algorithms. *Advances in Neural Information Processing Systems*, 12, 1999.

[24] S Eben Li. *Reinforcement Learning for Sequential Decision and Optimal Control*. Springer Verlag, Singapore, 2023.

[25] Abdoulaye O Ly and Moulay Akhloufi. Learning to drive by imitation: An overview of deep behavior cloning methods. *IEEE Transactions on Intelligent Vehicles*, 6(2):195–209, 2020.

[26] Diganta Misra. Mish: A self regularized non-monotonic activation function. *arXiv preprint arXiv:1908.08681*, 2019.

[27] William Peebles and Saining Xie. Scalable diffusion models with transformers. In *Proceedings of the IEEE/CVF International Conference on Computer Vision*, pages 4195–4205, 2023.

[28] Baiyu Peng, Qi Sun, Shengbo Eben Li, Dongsuk Kum, Yuming Yin, Junqing Wei, and Tianyu Gu. End-to-end autonomous driving through dueling double deep q-network. *Automotive Innovation*, 4:328–337, 2021.

[29] Michael Psenka, Alejandro Escontrela, Pieter Abbeel, and Yi Ma. Learning a diffusion model policy from rewards via q-score matching. *arXiv preprint arXiv:2312.11752*, 2023.

[30] John Schulman, Sergey Levine, Pieter Abbeel, Michael Jordan, and Philipp Moritz. Trust region policy optimization. In *International Conference on Machine Learning*, pages 1889–1897. PMLR, 2015.

[31] John Schulman, Filip Wolski, Prafulla Dhariwal, Alec Radford, and Oleg Klimov. Proximal policy optimization algorithms. *arXiv preprint arXiv:1707.06347*, 2017.

[32] David Silver, Guy Lever, Nicolas Heess, Thomas Degris, Daan Wierstra, and Martin Riedmiller. Deterministic policy gradient algorithms. In *International Conference on Machine Learning*, pages 387–395. Pmlr, 2014.

[33] Jascha Sohl-Dickstein, Eric Weiss, Niru Maheswaranathan, and Surya Ganguli. Deep unsupervised learning using nonequilibrium thermodynamics. In *International Conference on Machine Learning*, pages 2256–2265. PMLR, 2015.

[34] Yang Song, Conor Durkan, Iain Murray, and Stefano Ermon. Maximum likelihood training of score-based diffusion models. *Advances in Neural Information Processing Systems*, 34:1415–1428, 2021.

[35] Yang Song and Stefano Ermon. Generative modeling by estimating gradients of the data distribution. *Advances in Neural Information Processing Systems*, 32, 2019.

[36] Yang Song, Jascha Sohl-Dickstein, Diederik P Kingma, Abhishek Kumar, Stefano Ermon, and Ben Poole. Score-based generative modeling through stochastic differential equations. *arXiv preprint arXiv:2011.13456*, 2020.

[37] Richard S Sutton and Andrew G Barto. *Reinforcement learning: An introduction*. MIT press, 2018.

[38] Emanuel Todorov, Tom Erez, and Yuval Tassa. Mujoco: A physics engine for model-based control. In *Intelligent Robots and Systems*, 2012.

[39] Hado Van Hasselt, Arthur Guez, and David Silver. Deep reinforcement learning with double q-learning. In *Proceedings of the AAAI conference on artificial intelligence*, volume 30, 2016.

[40] Ashish Vaswani, Noam Shazeer, Niki Parmar, Jakob Uszkoreit, Llion Jones, Aidan N Gomez, Łukasz Kaiser, and Illia Polosukhin. Attention is all you need. *Advances in Neural Information Processing Systems*, 30, 2017.

- [41] Wenxuan Wang, Yuhang Zhang, Jiaxin Gao, Yuxuan Jiang, Yujie Yang, Zhilong Zheng, Wenjun Zou, Jie Li, Congsheng Zhang, Wenhan Cao, et al. Gops: A general optimal control problem solver for autonomous driving and industrial control applications. *Communications in Transportation Research*, 3:100096, 2023.
- [42] Zhendong Wang, Jonathan J Hunt, and Mingyuan Zhou. Diffusion policies as an expressive policy class for offline reinforcement learning. *The Eleventh International Conference on Learning Representations*, 2023.
- [43] Saining Xie Xinlei Chen, Zhuang Liu and Kaiming He. Deconstructing denoising diffusion models for self-supervised learning. *arXiv preprint arXiv:2401.14404*, 2024.
- [44] Long Yang, Zhixiong Huang, Fenghao Lei, Yucun Zhong, Yiming Yang, Cong Fang, Shiting Wen, Binbin Zhou, and Zhouchen Lin. Policy representation via diffusion probability model for reinforcement learning. *arXiv preprint arXiv:2305.13122*, 2023.
- [45] Ruihan Yang, Prakhar Srivastava, and Stephan Mandt. Diffusion probabilistic modeling for video generation. *Entropy*, 25(10):1469, 2023.

A Environmental Details

A.1 Experimental Environment Introduction

The benchmark tasks utilized in this study are depicted in Fig. 6, including Humanoid-v3, Ant-v3, HalfCheetah-v3, Walker2d-v3, InvertedDoublePendulum-v3, Hopper-v3, Pusher-v2, and Swimmer-v3.

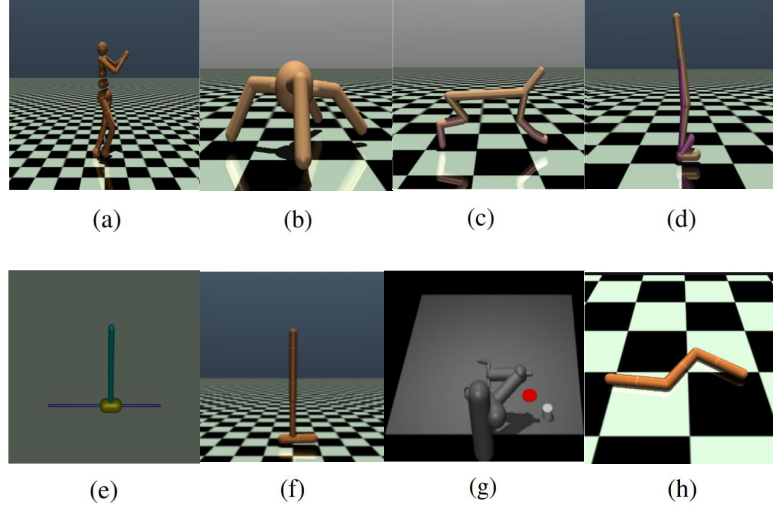


Figure 6: **Simulation tasks.** (a) Humanoid-v3: $(s \times a) \in \mathbb{R}^{376} \times \mathbb{R}^{17}$. (b) Ant-v3: $(s \times a) \in \mathbb{R}^{111} \times \mathbb{R}^8$. (c) HalfCheetah-v3 : $(s \times a) \in \mathbb{R}^{17} \times \mathbb{R}^6$. (d) Walker2d-v3: $(s \times a) \in \mathbb{R}^{17} \times \mathbb{R}^6$. (e) InvertedDoublePendulum-v3: $(s \times a) \in \mathbb{R}^6 \times \mathbb{R}^1$. (f) Hopper-v3: $(s \times a) \in \mathbb{R}^{11} \times \mathbb{R}^3$. (g) Pusher-v2: $(s \times a) \in \mathbb{R}^{23} \times \mathbb{R}^7$. (h) Swimmer-v3: $(s \times a) \in \mathbb{R}^8 \times \mathbb{R}^2$.

A.2 Training Details on MuJoCo tasks

Mujoco [38] is a simulation engine primarily designed for research in RL and robotics. It provides a versatile, physics-based platform for developing and testing various RL algorithms. Core features of Mujoco include a highly efficient physics engine, realistic modeling of dynamic systems, and support for complex articulated robots. Currently, it is one of the most recognized benchmark environments for RL and continuous control.

The hyperparameters of all baseline algorithms are shown in Table 2. Moreover, the hyperparameters of the DACER in the MuJoCo task are shown in Table 3.

B Limitation and Future Work

In this study, we propose using GMM to estimate the entropy of the diffusion policy and, based on this estimate, learn a parameter α to balance exploration and exploitation. However, the process of estimating entropy requires a large number of samples and takes a long time (about 40 ms). Therefore, we estimate the entropy of diffusion policy every 10,000 iterations to reduce the impact on training time. But, this approach prevents perfect integration with maximizing entropy RL. In future work, we will avoid using batch-size data to estimate entropy and find a balance between estimation accuracy and computational efficiency so as to better combine our method with maximizing entropy RL.

C Positive and Negative Social Impact

In this paper, we propose DACER, an online RL algorithm that uses the reverse diffusion process as a policy approximator. Diffusion policy has powerful multimodal representation capabilities, making it widely applicable in complex environments such as automated manufacturing, autonomous

TABLE 2
DETAILED HYPERPARAMETERS.

Hyperparameters	Value
<i>Shared</i>	
Replay buffer capacity	1000000
Buffer warm-up size	30000
Batch size	256
Initial alpha α	0.272
Action bound	$[-1, 1]$
Hidden layers in critic network	[256, 256, 256]
Hidden layers in actor network	[256, 256, 256]
Activation in critic network	GELU
Activation in actor network	GELU
Optimizer	Adam ($\beta_1 = 0.9, \beta_2 = 0.999$)
Actor learning rate	1e-4
Critic learning rate	1e-4
Discount factor (γ)	0.99
Policy update interval	2
Target smoothing coefficient (ρ)	0.005
Reward scale	0.2
<i>Maximum-entropy framework</i>	
Learning rate of α	3e-4
Expected entropy ($\bar{\mathcal{H}}$)	$\bar{\mathcal{H}} = -\dim(\mathcal{A})$
<i>Deterministic policy</i>	
Exploration noise	$\epsilon \sim \mathcal{N}(0, 0.1^2)$
<i>Off-policy</i>	
Replay buffer size	1×10^6
Sample batch size	20
<i>On-policy</i>	
Sample batch size	2000
Replay batch size	2000

driving, and industrial control. However, DACER could also enhance the exploratory capabilities and operational efficiency of military AI, potentially posing threats to citizen privacy and security.

TABLE 3
ALGORITHM HYPERPARAMETER

Parameter	Setting
Replay buffer capacity	1000000
Buffer warm-up size	30000
Buffer warm-up size (Humanoid, HalfCheetah)	200000
Batch size	256
Discount γ	0.99
Initial alpha α	0.27
Target network soft-update rate ρ	0.005
Network update times per iteration	1
Action bound	$[-1, 1]$
Reward scale	0.2
Hidden layers in noise prediction network	[256, 256, 256]
Hidden layers in noise prediction network (Humanoid)	[512, 512, 512]
Hidden layers in critic network	[256, 256, 256]
Activations in critic network	GeLU
Activations in actor network	Mish
Policy act distribution	TanhGauss
Policy min log std	-20
Policy max log std	0.5
Policy delay update	2
Number of Gaussian distributions for mixing	4
Number of action samples in entropy estimation	200
Alpha delay update	10000
Noise scale λ	0.1
Noise scale λ (Humanoid, HalfCheetah)	0.15
Optimizer	Adam
Actor learning rate	$1 \cdot 10^{-4}$
Critic learning rate	$1 \cdot 10^{-4}$
Alpha learning rate	$3 \cdot 10^{-2}$
Target entropy	$-\dim(\mathcal{A})$